Periodic Trajectories of Mobile Robots

Alexandra Q. Nilles, Israel Becerra and Steven M. LaValle

***Abstract*— Differential drive robots, such as robotic vacuums, often have at least two motion primitives: the ability to travel forward in straight lines, and rotate in place upon encountering a boundary. They are often equipped with simple sensors such as contact sensors or range finders, which allow them to measure and control their heading angle with respect to environment boundaries. We aim to find minimal control schemes for creating stable, periodic "patrolling" dynamics for robots that drive in straight lines and "bounce" off boundaries at controllable angles. As a first step toward analyzing high-level mobile robot dynamics in more general environments, we analyze the location and stability of periodic orbits in regular polygons. The contributions of this paper are: 1) proving the existence of periodic trajectories in n-sided regular polygons and showing the range of bounce angles that will produce such trajectories; 2) an analysis of their stability and robustness to modeling errors; and 3) a closed form solution for the points where the robot collides with the environment boundary while patrolling. We present simulations confirming our theoretical results.**

I. INTRODUCTION

Consider the path that a differential-drive mobile robot takes as it navigates a room. This robot has two motion primitives that it can execute reliably: moving in a straight line and turning in place. We can equip the robot with sensors that allow it to determine whether it is in contact with an environmental boundary and measure its heading relative to that boundary.

The main question addressed by this work is: *can we guarantee that the robot **patrols** a space on a repeatable, periodic path?* If so, what are the sensing and actuation requirements of this task? A better understanding of this common robotic task could lead to robots that are robust in the face of noise and complicated environments. Robots with robust patrolling behavior have applications such as monitoring environmental conditions in labs, warehouses, or greenhouses, where a few fixed sensors may not give adequate information.

Existing techniques for producing repeatable motion patterns for mobile robots involve equipping the robots with high-resolution sensors such as cameras, and using algorithms such as simultaneous localization and mapping (SLAM) to compute a map of the space and estimate the robot's state [1], [2], [3]. However, these robots can be expensive, require a large amount of computational and electrical power, and their accuracy can be impacted by changing environmental conditions (such as low light). In situations which require high-resolution mapping and localization in dynamic environments these tradeoffs are clearly worthwile. However, tasks such as monitoring humidity or temperature in a warehouse require only repeatable orbits in a relatively simple space, and some guarantees about what parts of the space will be covered. Robots with minimal sensing, actuation and control requirements will be more reliable and efficient at such tasks. Our approach requires precise knowledge about the structure of the environment, but does not require observation or calculation of the exact position of the robot. Such tradeoffs are common in robots, and allow us to optimize robotic designs for specific tasks and constraints.

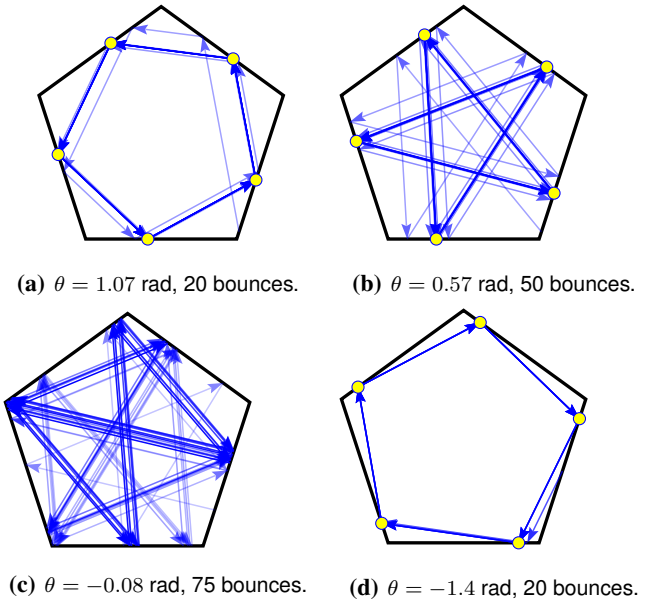

(a) $\theta = 1.07$ rad, 20 bounces. **(b)** $\theta = 0.57$ rad, 50 bounces.

(c) $\theta = -0.08$ rad, 75 bounces. **(d)** $\theta = -1.4$ rad, 20 bounces.

Fig. 1: Different behaviors of bounce trajectories in a regular pentagon. Older bounces become 2% more transparent with each new bounce. The circle on the boundary indicates the starting point of the trajectory. Figure (c) shows that periodic orbits are not guaranteed for all bounce angles.

The key approach of this work is treating the robot as a dynamical system defined by its motion primitives, independent of the hardware implementation. The contributions of this paper are 1) proving the existence of periodic orbits in n-sided regular polygons, and showing the range of bounce angles that will produce periodic orbits; 2) an analysis of these orbits, showing their stability and robustness; and 3) an analytic solution of the locations where the robot collides with the environment while in these orbits.

This paper is organized as follows: Section II describes related work. Section III presents the model definition and

A. Nilles, I. Becerra and S. M. LaValle are with the Department of Computer Science, University of Illinois at Urbana-Champaign. Urbana, IL 61801, USA. {nilles2,israelb4,lavalle}@illinois.edu

some useful concepts from dynamical systems. Section IV analyzes the case where the robot is constrained to bounce between sequential edges of the polygon, and we prove the existence and location of a periodic path using a fixed point technique. Section V generalizes this approach to find periodic paths of period k in regular n-gons, when k divides n. Section VII discusses possible extensions of this work, including to more generalized polygonal environments, and remaining open questions. By providing strong guarantees in the case of regular polygonal environments, we hope to lay the groundwork for analysis of more complex environments.

II. RELATED WORK

This dynamical system is closely related to mathematical billiards [4]. In billiards, an agent travels in a straight line until contacting a boundary of its environment, then bounces so that the incident angle is related to the outgoing angle by $\theta_o = -\theta_i$ (*specular* bouncing, such as how a laser beam reflects off mirrors). Our system generalizes this model by allowing the robot to control the angle of reflection.

There has been significant progress in generalizations of the billiards model: for example, *pinball billiards* is a model where the agent is deflected toward the normal with each bounce, $\theta_o = -\gamma\theta_i$ for $0 \leq \gamma \leq 1$. If the agent always bounces at the normal vector ($\gamma = 0$), this is called *slap billiards*. Work in this area focuses on analyzing the existence and structure of attractors [5] [6]. Additionally, [7] looks at the knots formed by periodic billiards in rectangular prisms. They generalize the idea of a constant-angle bounce to three dimensions, motivated by the behavior of Paramecium. They show that knots formed by constant bounces of $\pi/4$ in a rectangular prism are equivalent to billiard knots in a cube. Our study is in two dimensions and focuses on the necessary conditions for periodic orbits.

We are also inspired by work on map dynamics in polygons such as [8] and [9]. Also related is work on the combinatorial complexity of the region visited by specular bouncing ("visibility with reflection") in simple polygons [10]. There, the authors show the combinatorial complexity of the region touched after k bounces and provide a near-optimal algorithm for computing the region. Our work differs by analyzing non-specular bouncing and the effects of environment geometry. Specifically, we focus on determining regions of minimal complexity.

In [11], the authors describe a controller which generates chaotic dynamics in the heading of a mobile robot, guaranteeing that it will scan an entire connected workpace. Similarly to this work, their implementation requires a measurement of the local normal of boundaries upon contact. While the underlying dynamics are different, this work also treats the robot as a dynamical system over the workspace and leverages the results for useful patrolling behavior.

The motion primitives described in this paper are feasibly implemented on actual robots - in [12], the authors describe a differential-drive robot with bump and infrared range sensors which executes the same type of "bounces" described in this paper with error less than $\pm 10^\circ$. In that work, the authors developed an algorithm for navigation with such a robot; similarly, we show that patrolling is possible, and provide bounds on how much noise can be tolerated. Similarly, wall following robots [13], [14] are often capable of the motion primitives we describe - this work could help extend the capabilities of such robots with new motion strategies for patrolling the interior of a space.

A. Prior Work

In [15], the authors characterized some of the long-term dynamics of this dynamical system. They showed that the robot will have an orbit of period two between parallel edges, and the robot will move monotonically "outward" from acute vertices or edges that would meet in an acute vertex if extended to their intersection.

The authors in [15] defined distance- and link-unbounded segments as regions of the boundary where the robot may travel an unbounded distance or bounce an unbounded number of times. That work describes an algorithm for classifying the boundary of an arbitrary polygon into distance- and link-unbounded segments. However, the algorithm will not terminate when the robot's trajectory converges to a periodic orbit, since in this case the distance- and link-unbounded regions shrink to points on the polygon boundary, such as in Figures 1a and 1b.

One purpose of this paper is to begin to identify cases where the dynamical system's attractor is a set of separate points, not intervals, on the environment boundary. The algorithm in [15] can be used only for environments with attractors that are segments on the boundary, for which the algorithm is guaranteed to terminate.

III. MODEL DEFINITION

A point robot moves in a bounded subset of the plane P, defined by a continuous boundary δP. For most of this discussion, the environment will be a simple regular polygon, so δP is an n-gon with n straight edges intersecting at n vertices $(v_0, v_1, \ldots, v_{n-1})$. An edge of the polygon is represented as $v_i v_{i+1}$.

The robot drives in a straight line until encountering δP. It then rotates until its heading is at an angle θ clockwise of the inward-facing boundary normal, where $-\pi/2 < \theta < \pi/2$. Then the robot repeats this procedure indefinitely. Figure 2 shows two sample bounces, at angles θ^+ and θ^-.

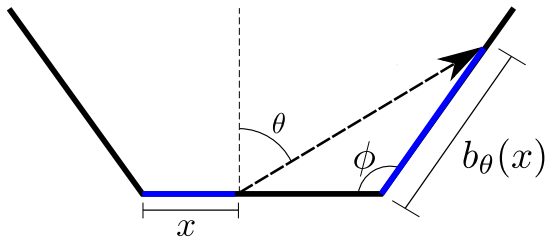

Fig. 2: A sample bounce, showing θ measured clockwise from the normal. The other labels show the geometric meaning of the bounce map defined in Lemma 1.

The function that these actions define between points on δP is $B_\theta : \delta P \to \delta P$, defining our dynamical system. We will refer to this function as the *bounce map*, in the same spirit as the *logistic map* in discrete dynamical systems, not to be confused with a map of the environment. When the bounce map is iterated k times, we write B_θ^k. B_θ is not well defined on vertices of δP, so we will not consider trajectories which reach a vertex.

A sequence of points $[p_0, \ldots, p_k]$ is a *flow* of B_θ if $p_i = B_\theta(p_{i-1})$ for $1 \leq i \leq k$. A flow is an *orbit* with *period* k if $B_\theta(p_{k-1}) = p_0$. A *limit cycle* is an orbit where nearby flows tend asymptotically toward or away from the orbit [16].

IV. BOUNCING TO ADJACENT EDGE

Take a regular n-gon with boundary δP, each side of length l, and each interior angle of $\phi = (n-2)\pi/n$ radians [17]. In simulation, for some values of θ we observe stable orbits that bounce off each adjacent edge (Figure 1a). To analyze these orbits, we imagine that B_θ is constrained to send the robot from edge $v_i v_{i+1}$ to edge $v_{i+1}v_{i+2}$ for all bounces, and then solve for the conditions necessary to guarantee this behaviour.

We begin our analysis by presenting a trigonometric function (Lemma 1) that is used to determine the existence and location of a periodic path. Lemma 2 establishes the conditions under which that function is a contraction mapping with a unique fixed point. A fixed point of this mapping function corresponds to a stable orbit that has the shape of a regular n-gon, inscribed in δP. Finally, Proposition 1 presents a closed form solution for the fixed point that allows us to locate where the robot collides with the polygon in these stable orbits.

Lemma 1: Assume that the robot bounces at angle θ to the next adjacent edge in a counterclockwise (positive) direction. Under this condition, define the constrained bounce map $b_\theta^+ : (0, l) \to (0, l)$ which takes x, the robot's distance from vertex v_i, and maps it to $b_\theta^+(x)$, the resulting distance from vertex v_{i+1}. This mapping function is given by

$$b_\theta^+(x) = c(\theta)(l - x), \tag{1}$$

in which $c(\theta) = cos(\theta)/cos(\theta - \phi)$.

Proof: Using the triangle formed by two adjacent edges and the robot's trajectory between them (see Fig 2), we can solve for b_θ^+. The law of sines establishes that

$$\frac{b_\theta^+(x)}{\sin(\pi/2 - \theta)} = \frac{l - x}{\sin(\pi - (\pi/2 - \theta) - \phi)}$$

which we can rewrite as

$$b_\theta^+(x) = \frac{\cos(\theta)}{\cos(\theta - \phi)}(l - x) = c(\theta)(l - x).$$

■

Lemma 2: If $|c(\theta)| < 1$, then $b_\theta^+(x)$ is a contraction mapping and has a unique fixed point.

Proof: We take $(0, l)$ to be a metric space with metric $d(x, y) = |y - x|$. To be a contraction mapping, b_θ^+ must satisfy

$$d(b_\theta^+(x), b_\theta^+(y)) \leq k d(x, y)$$

for all $x, y \in (0, l)$ and some nonnegative real number $0 \leq k < 1$.

When we check this property, we see that

$$\begin{aligned} d(b_\theta^+(x), b_\theta^+(y)) &= |c(\theta)(l - y) - c(\theta)(l - x)| \\ &= |c(\theta)(x - y)| \\ &= |c(\theta)| d(x, y). \end{aligned}$$

Thus if $|c(\theta)| < 1$, then b_θ^+ is a contraction mapping, and by the Banach fixed-point theorem, it has a unique fixed point [18]. ■

Corollary 1: At the fixed point, b_θ^+ represents the robot bouncing from a point that is distance x_{FP} from vertex v_i, to a point that is distance x_{FP} from vertex $v_{(i+1) \bmod n}$, for all $i \in [0, \ldots, n-1]$. Thus, a fixed point of b_θ^+ implies an orbit of B_θ.

Remark 1: Note that the proof of Lemma 2 holds for all $x, y \in (0, l)$, so it does not matter where the robot starts bouncing, implying that this orbit is a stable limit cycle of the dynamical system, with the largest possible region of stability.

Proposition 1: In every regular n-sided polygon with side length l and interior angle ϕ, there exists a range for θ such that iterating $B_\theta(x)$ on any $x \in \delta P$ results in a stable limit cycle of period n, which strikes the boundary at points that are distance x_{FP} from the nearest clockwise vertex. x_{FP} is given by

$$x_{FP} = \begin{cases} \frac{lc(\theta)}{1+c(\theta)} & \phi/2 < \theta < \pi/2 \\ \frac{l}{1+c(\theta)} & -\pi/2 < \theta < -\phi/2 \end{cases} \tag{2}$$

in which $c(\theta) = cos(\theta)/cos(\theta - \phi)$.

Proof: In a regular n-sided polygon with side length l, let the robot begin its trajectory at a point $p \in P$ which is at a distance x from the nearest vertex in the clockwise direction. We will begin by constraining the robot to bounce counterclockwise, at an angle $0 < \theta < \pi/2$ such that it strikes the nearest adjacent edge, such as in Figure 1a. The function b_θ^+ given in Lemma 1 describes such bouncing behaviour.

By Lemma 2, $b_\theta^+(x)$ has a unique fixed point, which is an orbit of B_θ since the robot is contacting each edge at the same distance from the vertex at each bounce. By iterating the map b_θ^+, we can explicitly find the value of the fixed point, and thus the points on δP touched by the robot in its orbit. Iterating b_θ^+ k times yields

$$\begin{aligned} {b_\theta^+}^k(x) &= c(\theta)(l - c(\theta)(l - \ldots c(\theta)(l - x)\ldots)) \\ &= \sum_{i=1}^{k} (-l)(-c(\theta))^i + (-c(\theta))^k x \end{aligned}$$

and taking the limit as $k \to \infty$ and shifting the index gives

$${b_\theta^+}^\infty(x) = l + \sum_{i=0}^{\infty} (-l)(-c(\theta))^i$$

.

Note that the starting position, x, drops out when the limit is taken - the orbit converges regardless of starting position. The sum is geometric, and since $|c(\theta)| < 1$ (the condition stated in Lemma 2), the fixed point (for counterclockwise orbits) becomes

$$(b_\theta^+)^\infty(x) = \frac{lc(\theta)}{1+c(\theta)}$$

.

So the trajectory of a robot with bounce angle θ satisfying $|c(\theta)| < 1$ converges to a limit cycle in the shape of an inscribed n-gon, with collision points x_{FP} at distance $(lc(\theta))/(1+c(\theta))$ from the nearest vertex in the clockwise direction. When this calculation is redone for bounces in the counterclockwise direction ($-\pi/2 < \theta < 0$), the resulting fixed point x_{FP} is $l/(1+c(\theta))$. Moreover, since $c(\theta) \in (0,1)$ for stable orbits, and considering the past two expressions for x_{FP}, we find that the fixed point x_{FP} for bounces can take all values in $(0,l)$ except for $l/2$, which would require $c(\theta) = 1$.

Next, we examine the stability condition, $|\frac{\cos(\theta)}{\cos(\theta-\phi)}| < 1$. Since $0 < \theta < \pi/2$ for b_θ^+, $\cos(\theta)$ is always positive, then we must have $|\cos(\theta-\phi)| > \cos(\theta)$, from where we can obtain the range $\phi/2 < \theta < \pi/2$. Likewise, in the clockwise direction, $-\pi/2 < \theta < 0$ yields $-\pi/2 < \theta < -\phi/2$. Thus, we have a guarantee on the range of bounce angles that will result in periodic orbits, starting from any point on the polygon's boundary. ■

Remark 2: Note that calculating the Lyapunov exponent [16] for the map $b_\theta(x)$ gives the same result: $|db_\theta(x)/dx| = |c(\theta)|$, which implies that $|c(\theta)| < 1$ gives a stable fixed point.

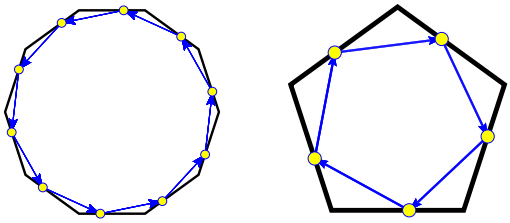

Fig. 3: Simulated orbits for adjacent edge bouncing in regular polygons. Predicted collision points are indicated by circles. Both simulations are of the trajectory after 300 bounces from an arbitrary start point.

V. GENERALIZATION

Instead of bouncing between adjacent edges, we may ask what happens when the robot bounces between edge v_0v_1 and edge v_mv_{m+1}, "skipping" $m-1$ edges, such as in Figure 1b where the robot bounces off every other edge.

Proposition 2 states the existence of a stable limit cycle with period k in every regular n-sided polygon, in the particular case where $k|n$. Then, following a similar approach as in Section IV, we prove in Lemma 4 that the trigonometric function of Lemma 3 is a contraction mapping with a unique fixed point, and conclude with Theorem 3 presenting a closed form solution for the fixed point (hence the location of the stable orbit) when the robot bounces skipping $m-1$ edges.

Proposition 2: In every regular n-sided polygon, there exists a stable limit cycle with period k for all k such that $k > 2$ and $k|n$.

Proof: For all prime $n \geq 3$, the statement is true by Proposition 1, since $k = n$ for $k|n$, and Proposition 1 guarantees a stable limit cycle that strikes each edge sequentially.

Now consider any non-prime $n > 3$, and assume $k > 2$ to avoid trajectories between parallel edges (addressed in [15]). Proposition 1 guarantees a stable limit cycle that strikes each edge of an n-sided polygon sequentially. For all k such that $k|n$, we can choose k edges of the n-gon such that the edges are equally spaced. We can then imagine extending these edges to their intersection points, forming a regular k-gon. By Proposition 1, the bounce map in this regular k-gon is guaranteed to induce a stable limit cycle, with collision points at parameter x_{FP} on the edge for all x_{FP} except the very center point of the edge. Thus θ can be chosen such that the bounce map sends the robot to every (n/k)- *th* edge such that the trajectory will converge to a stable cycle with period k. The result follows. ■

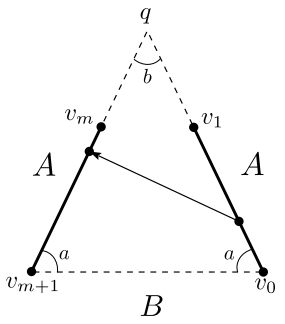

Fig. 4: A bounce from edge v_0v_1 to edge v_mv_{m+1}. The other edges of the polygon are not drawn, and the distance between the edges is not to scale.

Lemma 3: Assume that B_θ is constrained so the robot "skips" $m-1$ edges with each bounce in a counterclockwise direction. This constrained bounce map $b_{\theta,m}^+ : (0,l) \to (0,l)$, which takes x (the robot's distance from vertex v_i) and maps it to $b_{\theta,m}^+(x)$ (the resulting distance from vertex v_{i+m}) is given by

$$b_{\theta,m}^+(x) = c(\theta)(A-x) + l - A, \tag{3}$$

in which $c(\theta)$ is generalized to

$$c(\theta) = \cos(\theta)/\cos\left(\theta - \frac{\pi(n-2m)}{n}\right) \tag{4}$$

and

$$A = \frac{l\sin(\frac{\pi(m+1)}{n})\sin(\frac{m\pi}{n})}{\sin(\frac{\pi}{n})\sin(\frac{\pi(n-2m)}{n})}. \tag{5}$$

Proof: Let $m \leq \lfloor n/2 \rfloor$ - the robot bounces counterclockwise. Without loss of generality assume that we start

on edge v_0v_1. Extend the line segments v_0v_1 and v_mv_{m+1} to their point of intersection q, forming the triangle $v_0v_{m+1}q$. Let $a = \angle qv_{m+1}v_0 = \angle qv_0v_{m+1}$, by symmetry. Let $b = \angle v_{m+1}qv_0$. Let $A = |qv_{m+1}| = |qv_0|$ and $B = |v_{m+1}v_0|$ (see Figure 4). Each of the sides of the polygon has length l, and the robot begins its trajectory at a point which is distance x from v_0. We wish to find $b^+_{\theta,m}(x)$, the distance from the endpoint of the bounce to point v_m.

By the law of sines, we have

$$A = \frac{B\sin(a)}{\sin(b)}$$

We can then form the triangle from the points v_0, v_{m+1}, and the center of the regular n-gon. The distance from the center of a regular n-gon to any of its vertices is $\frac{l}{2\sin(\pi/n)}$ [17]. The angle subtended by the edges v_0v_1 through v_mv_{m+1} is $2\pi(m+1)/n$. Thus, B becomes

$$B = \frac{l\sin(\pi(m+1)/n)}{\sin(\pi/n)}$$

.

The angle a can be found by considering the polygon formed by edges v_0v_1 through v_mv_{m+1}, closed by edge $v_{m+1}v_0$. This polygon has $m+2$ vertices, so its angle sum is $m\pi$. m of these vertices have the vertex angle of the regular n-gon, $(n-2)\pi/n$. The remaining two vertices have angle a. Therefore, $2a + m(n-2)\pi/n = m\pi$, so $a = m\pi/n$, and thus

$$A = \frac{l\sin(\frac{\pi(m+1)}{n})\sin(\frac{m\pi}{n})}{\sin(\frac{\pi}{n})\sin(\frac{\pi(n-2m)}{n})}$$

.

Using the triangle formed by the the bounce of the robot and vertex q, the law of sines states

$$\frac{A-x}{\sin(\theta - \pi/2 + (2\pi m)/n)} = \frac{A - l + b^+_{\theta,m}(x)}{sin(\pi/2-\theta)},$$

which we rewrite as

$$b^+_{\theta,m}(x) = \frac{(A-x)\cos(\theta)}{\cos(\theta - \frac{\pi(n-2m)}{n})} + l - A$$

$$= c(\theta)(A-x) + l - A.$$

■

Lemma 4: If $|c(\theta)| < 1$, then $b^+_{\theta,m}(x)$ is a contraction mapping, and therefore has a unique fixed point.

Proof: We take $(0, l)$ to be a metric space with metric $d(x, y) = |y - x|$. To be a contraction mapping, $b^+_{\theta,m}$ must satisfy

$$d(b^+_{\theta,m}(x), b^+_{\theta,m}(y)) \leq kd(x, y)$$

for all $x, y \in (0, l)$ and some nonnegative real number $0 \leq k < 1$.

When we check this property, we see that

$$\begin{aligned} d(b^+_{\theta,m}(x), b^+_{\theta,m}(y)) &= |b^+_{\theta,m}(x) - b^+_{\theta,m}(y)| \\ &= |c(\theta)(A-x) + l - A - \\ &\quad c(\theta)(A-y) - l + A| \\ &= |c(\theta)(y-x)| \\ &= |c(\theta)|d(x, y). \end{aligned}$$

Thus if $|c(\theta)| < 1$, then $b^+_{\theta,m}$ is a contraction mapping, and by the Banach fixed-point theorem has a unique fixed point [18]. ■

Theorem 3: In every regular n-sided polygon with side length l and interior angle $(n-2)\pi/n$, there exists a range for θ such that iterating $B_\theta(x)$ on any $x \in \delta P$, results in a stable limit cycle that strikes the boundary skipping $m-1$ edges, and strikes at points that are distance x_{FP} from the nearest clockwise vertex, with x_{FP} given by

$$x_{FP} = \begin{cases} \frac{l - A(1-c(\theta))}{1+c(\theta)}, & \frac{\phi_m}{2} < \theta < \frac{\phi_{m-1}}{2} \\ \frac{lc(-\theta) + A(1-c(-\theta))}{1+c(-\theta)}, & \frac{-\phi_{m-1}}{2} < \theta < \frac{-\phi_m}{2} \end{cases} \quad (6)$$

in which $c(\theta)$ and A are given by Equations (4) and (5) respectively, and $\phi_m = \frac{\pi(n-2m)}{n}$.

Proof: Consider an n-sided polygon with side length l and let the robot begin its trajectory at a point $p \in \delta P$ which is at a distance x from the nearest vertex in the clockwise direction. We begin by assuming the robot bounces in the conterclockwise direction, at an angle θ such that instead of bouncing between adjacent edges the robot "skips" $m-1$ edges. The function $b^+_{\theta,m}(x)$ in Lemma 3 obeys such bouncing behaviour.

By Lemma 4, the map $b^+_{\theta,m}(x)$ has a unique fixed point, which implies an orbit of B_θ. By iterating the map $b^+_{\theta,m}(x)$, we explicitly find the value of the fixed point x_{FP}, and thus the points on δP touched by the robot in its orbit. After k iterations, this mapping function becomes

$$b^+_{\theta,m}{}^k(x) = \sum_{i=0}^{k-1}(-c(\theta))^i(l - A(1-c(\theta))) + (-c(\theta))^k x$$

and after taking the limit as $k \to \infty$, and considering $|c(\theta)| < 1$ (the condition stated in Lemma 4), we find the fixed point to be

$$b^+_{\theta,m}{}^\infty(x) = \frac{l - A(1-c(\theta))}{1+c(\theta)} \quad (7)$$

So we expect every converging counterclockwise periodic orbit which skips $m-1$ edges, $m \geq 1$, to collide with the environment at distance $\frac{l-A(1-c(\theta))}{1+c(\theta)}$ from the nearest clockwise vertex.

The clockwise case can be found by reflecting the polygon and the bounce over the y-axis, so the clockwise fixed point is given by $\frac{lc(-\theta)+A(1-c(-\theta))}{1+c(-\theta)}$, which is the second expression in Equation 6.

Next, examining the stability condition, $|c(\theta)| < 1$, with $c(\theta)$ given by Equation (4), and considering that $0 < \theta <$

$\pi/2$ for b_θ^+, we can obtain the range $\pi(n-2m)/2n < \theta < \pi(n-2(m-1))/2n$. Likewise, in the clockwise direction, $-\pi/2 < \theta < 0$ yields $-\pi(n-2(m-1))/2n < \theta < -\pi(n-2m)/2n$. Thus, we have a guarantee on the range of bounce angles that will result in periodic orbits, starting from any point on the polygon's boundary.

■

Remark 3: When $m = 1$ (agent skips no edges while bouncing around polygon), A reduces to l, and the expression for $b_{\theta,1}^+(x)$ reduces to $b_\theta^+(x)$ as in Equation 3, so Equation 3 is a special case of Equation 7. Furthermore, the bounds on θ also reduce to the bounds $\phi/2 < \theta < \pi/2$ and $-\phi/2 < \theta < -\pi/2$, where $\phi = \pi(n-2)/n$.

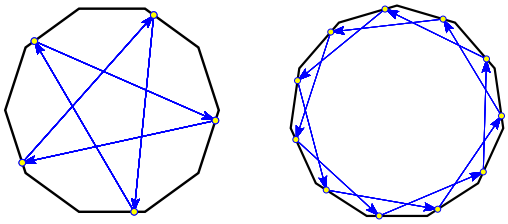

Fig. 5: Simulated orbits for generalized edge bouncing in regular polygons, with $n = 9, m = 4, \theta = -0.8$ rad and $n = 11, m = 2, \theta = 0.4$ rad. Predicted collision points are indicated by circles. Both simulations are of the trajectory after 300 bounces from an arbitrary start point.

A. Implications for Uncertainty in Implementations

All physical implementations of the required motion primitives will be imperfect - for example, differential drive robots can have asymmetries in the motors powering each wheel, which can result in a curved path through the interior of the environment, or an inaccurate rotation while aligning to θ. These differences between the model and the implementation produce a constant offset in the bounce angle, $\theta + \epsilon$. Theorem 3 gives a bound on the maximum allowable error in this situation, and suggests that random errors within this bound will still result in near-periodic orbits.

For each stable orbit in a given environment, we can use the bounds on $c(\theta)$ to determine the range of angles that will result in that orbit. Thus, when designing a "patrolling" robot in an environment with regular polygonal geometry, a robot designed to bounce at an angle θ in the center of one of these ranges ($\phi_m/2 < \theta < \phi_{m-1}/2$ or $-\phi_{m-1}/2 < \theta < -\phi_m/2$) will be maximally robust to actuator or sensor errors. The resulting maximum allowable error, ϵ_{max}, will be $\pm|(\phi_m - \phi_{m-1})/2|$. Bounces with error within this range will still result in stable orbits of the workspace, because the bounce still acts as a contraction mapping on the edge intervals.

However, these orbits will impact the boundary at different locations than expected. If there is a constant error in the bounce angle, so that the effective bounce angle is $\theta + \epsilon$, with $\epsilon < \epsilon_{max}$, the resulting difference in the location of the collision point on each edge will be $\Delta_x = b_{m,\theta+\epsilon}^\infty - b_{m,\theta}^\infty$.

VI. SIMULATIONS

The figures and experimental simulations for this paper were computed using a Haskell program which heavily used the *Diagrams* library [19]. The simulator can also be used for specular bouncing simulations, and could be of use to those studying classical billiards, or variants such as pinball billiards. It is also capable of simulating random bounces, or random noise on top of deterministic bouncing. Code is open source and on GitHub [1].

The purpose of the simulations is to confirm experimentally the theoretical results obtained in previous sections. Figure 3 depicts simulated orbits for adjacent edge bouncing after 300 bounces. Predicted collision points x_{FP} are indicated by circles. Figure 4 shows simulated orbits for two pairs of n and m values in the case where the robot bounces skipping $m-1$ edges. The trajectories after 300 bounces are displayed.

Note that the simulated orbits were computed by iteratively bouncing the robot in the environment from an arbitrary start point rather than just plotting the resulting orbit from the predicted collision points. In all simulations, the simulated collision points (tips of arrows) and the theorized collision points x_{FP} (circles) coincide.

Figure 6a shows three orbits simulated from different start points but with the same bouncing angle θ. Regardless of starting position, the same bouncing angle θ produces trajectories which converge to the same limit cycle, as stated in Remark 1.

As stated in Theorem 3 there exist ranges of θ that produce stable orbits when the robot skips $m-1$ edges with $m \geq 1$. For regular hexagons, $\pi/3$ is the lower bound on θ such that the robot strikes every edge sequentially, and the upper bound on θ such that the robot strikes every other edge. The orbits shown in Figure 6b were generated setting $\theta = \pi/3 \pm 0.05$. As predicted, one orbit bounces off every other edge, while the other strikes every sequential edge.

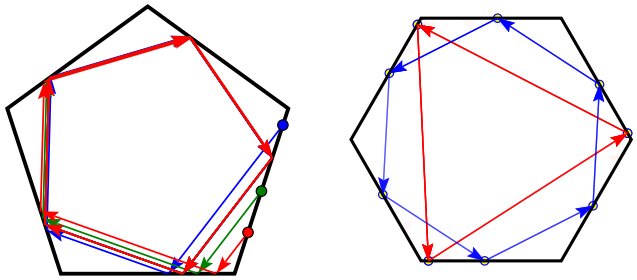

(a) Three orbits simulated with different start points - the three circles - but same bouncing angle θ. The limit cycle is the same.

(b) Two simulated orbits with the same start point but θ set to $\pi/3 + 0.05$ (blue) and $\pi/3 - 0.05$ (red). One skips no edges and the other skips one edge.

Fig. 6: Evidence from simulation that (a) limit cycles are independent of start position, and that (b) our predicted "transition angle" between striking every edge and every other edge is correct.

[1] https://github.com/alexandroid000/bounce

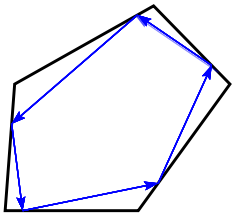

(a) A stable orbit in a sheared pentagon.

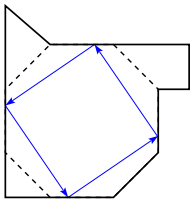

(b) A stable orbit in a nonconvex environment.

Fig. 7: Stable orbits also exist in non-regular polygons.

VII. CONCLUSIONS AND FUTURE WORK

In this paper we considered robots that drive in straight lines and bounce off boundaries at controllable angles. We analysed the location and stability of periodic orbits in regular polygons, which might be used to patrol the space on a repeatable, periodic path.

We first presented the case of stable orbits that bounce off each adjacent edge. We proved the existence of periodic orbits in n-sided regular polygons, and showed the range of bounce angles that will produce such orbits along with an analysis of their stability and robustness to modeling errors. We generalized our results to the case where the robot skips $m-1$ edges. In both cases we present a closed form solution for the locations where the robot collides with the environment boundary while patrolling.

The existence of periodic orbits along with the presented closed form solutions for x_{FP} show that it is possible to design a robust patrolling path for a given environment, using limited motion and sensing capabilities. These orbits have the useful properties of being robust to modelling errors and being independent of the start position.

One interesting line of research could be to explore how the convergence of these orbits could be used to narrow down the set of possible positions of the robot, in navigation and localization tasks.

The most pressing open question is how to extend the current analysis to non-regular polygons. In non-regular polygons, it is not clear how to solve for orbits as the fixed point of one mapping function. Yet, limit cycles still exist in other polygons, such as regular polygons under linear transformations, as seen in Figure 7a. It is worth mentioning that our current analysis can be used to design stable orbits in polygons with enough local similarity to regular polygons, such as in Figure 7b.

Another direction for future research is to consider a time-varying error $\epsilon(t)$ over θ. This would allow us to model external disturbances to the motion and sensing of the robot. In simulations we have noticed that if $\epsilon(t)$ does not cause $\theta \pm \epsilon(t)$ to exceed the bounds on θ that cause periodic orbits, the robot's trajectory stays within a certain range of the predicted collision points. A theoretical analysis of these observations would be useful.

ACKNOWLEDGMENT

This work is supported by NSF grant 1035345, NSF grant 1328018, and CONACyT post-doctoral fellowship 277028. The authors would like to thank Michael Zeng for his contributions to the fixed-point formulation of the problem.

REFERENCES

[1] M. G. Dissanayake, P. Newman, S. Clark, H. F. Durrant-Whyte, and M. Csorba, "A solution to the simultaneous localization and map building (slam) problem," *IEEE Transactions on robotics and automation*, vol. 17, no. 3, pp. 229–241, 2001.

[2] M. Montemerlo, S. Thrun, D. Koller, B. Wegbreit, *et al.*, "Fastslam: A factored solution to the simultaneous localization and mapping problem," in *Aaai/iaai*, 2002, pp. 593–598.

[3] H. Durrant-Whyte and T. Bailey, "Simultaneous localization and mapping: part i," *IEEE robotics & automation magazine*, vol. 13, no. 2, pp. 99–110, 2006.

[4] S. Tabachnikov, *Geometry and Billiards*. American Mathematical Society, 2005.

[5] R. Markarian, E. Pujals, and M. Sambarino, "Pinball billiards with dominated splitting," *Ergodic Theory and Dynamical Systems*, vol. 30, pp. 1757–1786, 2010.

[6] G. Del Magno, J. Lopes Dias, P. Duarte, J. P. Gaivão, and D. Pinheiro, "SRB measures for polygonal billiards with contracting reflection laws," *Communications in Mathematical Physics*, vol. 329, no. 2, pp. 687–723, 2014.

[7] V. Jones and J. Przytycki, "Lissajous knots and billiard knots," *Banach Center Publications*, vol. 42, no. 1, pp. 145–163, 1998.

[8] W. P. Hooper and R. E. Schwartz, "Billiards in nearly isosceles triangles," *Journal of Modern Dynamics*, vol. 3, no. 2, pp. 159–231, June 2013.

[9] R. Schwartz, "The pentagram map," *Experiment. Math.*, vol. 1, no. 1, pp. 71–81, 1992.

[10] B. Aronov, A. R. Davis, T. K. Dey, S. P. Pal, and D. C. Prasad, *Visibility with multiple reflections*. Berlin, Heidelberg: Springer Berlin Heidelberg, 1996, pp. 284–295.

[11] Y. Nakamura and A. Sekiguchi, "The chaotic mobile robot," *IEEE Transactions on Robotics and Automation*, vol. 17, no. 6, pp. 898–904, 2001.

[12] J. S. Lewis and J. M. O'Kane, "Planning for provably reliable navigation using an unreliable, nearly sensorless robot," *International Journal of Robotics Research*, vol. 32, no. 11, pp. 1339–1354, September 2013.

[13] R. Carelli and E. O. Freire, "Corridor navigation and wall-following stable control for sonar-based mobile robots," *Robotics and Autonomous Systems*, vol. 45, no. 3, pp. 235–247, 2003.

[14] A. G. Lamperski, O. Y. Loh, B. L. Kutscher, and N. J. Cowan, "Dynamical wall following for a wheeled robot using a passive tactile sensor," in *Proceedings of the 2005 IEEE International Conference on Robotics and Automation*, April 2005.

[15] L. H. Erickson and S. M. LaValle, "Toward the design and analysis of blind, bouncing robots," in *IEEE International Conference on Robotics and Automation*, 2013.

[16] E. Jackson, *Perspectives of Nonlinear Dynamics*. Cambridge University Press, 1992, vol. 1.

[17] R. Johnson, *Advanced Euclidean Geometry*, ser. Dover books on advanced mathematics. Dover Publications, 1929.

[18] A. Granas and J. Dugundji, *Elementary Fixed Point Theorems*. New York, NY: Springer New York, 2003, pp. 9–84.

[19] B. A. Yorgey, "Monoids: theme and variations (functional pearl)," in *ACM SIGPLAN Notices*, vol. 47, no. 12. ACM, 2012, pp. 105–116.